Electronic Supplementary Material (ESI) for Physical Chemistry Chemical Physics.

Ultrafast Structural Flattening Motion in Photoinduced Excited State Dynamics of a Bis(dimine) Copper(I) Complex

Likai Du[†‡§], Zhenggang Lan[*†‡§]

[†]Key Laboratory of Biobased Materials, Qingdao Institute of Bioenergy and Bioprocess Technology, Chinese Academy of Sciences, Qingdao, 266101, Shandong, People's Republic of China

[‡]University of Chinese Academy of Sciences, Beijing 100049, People's Republic of China

[§]The Qingdao Key Lab of Solar Energy Utilization and Energy Storage Technology,Qingdao Institute of Bioenergy and Bioprocess Technology, Chinese Academy of Sciences, Qingdao, 266101, Shandong, People's Republic of China.

* Author for correspondence: Fax: +86-532-80662778; Tel: +86-532-80662630;

E-mail: lanzg@qibebt.ac.cn

Supporting Information

1. Technical Details in the Trajectory Analysis

The calculation of interligand dihedral angle (φ) requires the definition of the molecular plane for the dmp ligand. Here, the planar equation of the single dmp ligand at a specific geometry was easily constructed, if we assume all atoms in the dmp ligand are approximately located on the same plane. With known planar equations, the definition of the interligand dihedral angle (φ) becomes a trial problem, which is dihedral angle between two dmp-ligand planes. Note that the hydrogen atoms are omitted in these analyses. In practice, we defined a planar equation for one dmp ligand as

$$Ax + By + Cz + D = 0 .$$

Then, the parameters of the above planar equation were directly obtained by the least-square fitting of the Cartesian coordinates of all atoms (except H) in one dmp ligand. The dihedral angle (φ, Fig. 2 in the main manuscript) between two planar equations was furtherly derived from the calculation of their normal vectors.

The planarity (or planar degree) of the single dmp ligand, could be measured by the residue of the atoms belonging to the dmp ligand away from the planar equation. We defined the out-of-plane deviation with the total residue distance (R):

$$R = \frac{1}{n} \sum_{i \in dmp} \left| Ax_i + By_i + Cz_i + D \right| ,$$

where n is the number of atoms in one dmp ligand, and i loops over each atom (except H) in one dmp ligand. As shown below (Figure. S10a), the planarity of the dmp ligand nearly remains during the evolution.

We also monitored the overall motion of one dmp ligand (Fig. 6b), that is defined as the dihedral angle between a dmp ligand plane at each time step with respect to the same plane at the initial frame of the dynamics. The same definition of the above planar equation was used in the analysis.

The Fourier transformation of the Cu-N bond length and N-Cu-N bond angle was performed for their data within one picosecond. This transformation was performed for each trajectory in our simulation, and then, the transformation results were averaged and given in Fig. 8.

2. Tables and Figures

Table S1. Selected geometric parameters calculated at DFT and TDDFT level with 6-31G* basis set for the optimized ground and low-lying excited state of the $[Cu(dmp)_2]^+$ complex.

	Cu-N (Å)[a]	N-Cu-N (°)[b]	DHA (°)[c]
CAM-B3LYP			
S_0	1.99	84.2	90.0
S_1	1.94, 2.07	86.9, 81.6	70.4
M06-2X			
S_0	2.06	81.9	90.0
S_1	1.94, 2.10	80.2, 86.4	68.8
BHandHLYP			
S_0	2.04	82.7	90.0
S_1	1.94, 2.10	80.5, 86.3	73.4

[a,b]For the excited state, the Cu-N bond length and N-Cu-N bond angle for each ligand is different, and mainly split into two groups.

[c]Dihedral Angle (DHA) between dmp ligands.

Table S2. The transition density analysis of the excitation between $[Cu(dmp)_2]^+$ cation (**C**) and PF_6^- anion (**A**) for the $[Cu(dmp)_2](PF_6)$ complex. Our results show minor contribution of anion to cation charge-transfer excitation for low-lying electronic states. Two blocks (the cation and anion) were used to build intra-unit and inter-unit transition probabilities.

	C→C	A→C	C→A	A→A
S_1	0.9981	0.0011	0.0008	0.0000
S_2	0.9981	0.0011	0.0008	0.0000
S_3	0.9982	0.0011	0.0007	0.0000

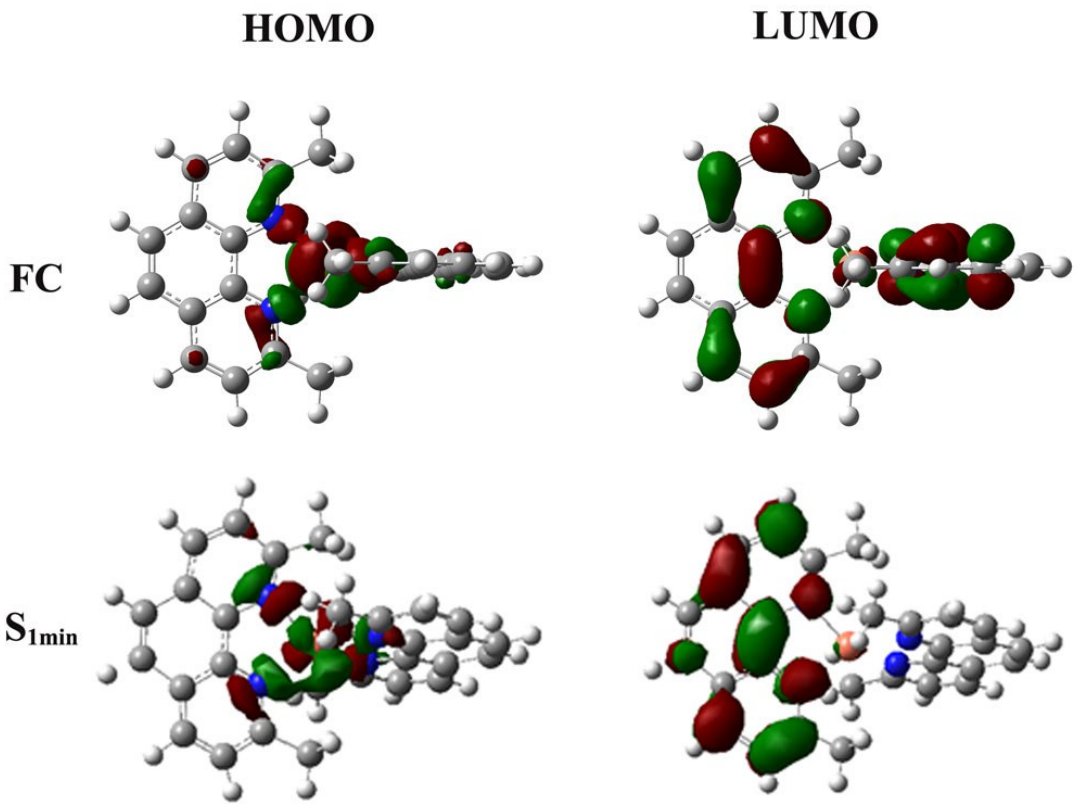

Fig. S1 HOMO and LUMO orbitals (S_1 state) at the Franck–Condon (FC) geometry (S_0 minimum) and the flattened geometry (S_1 minimum).

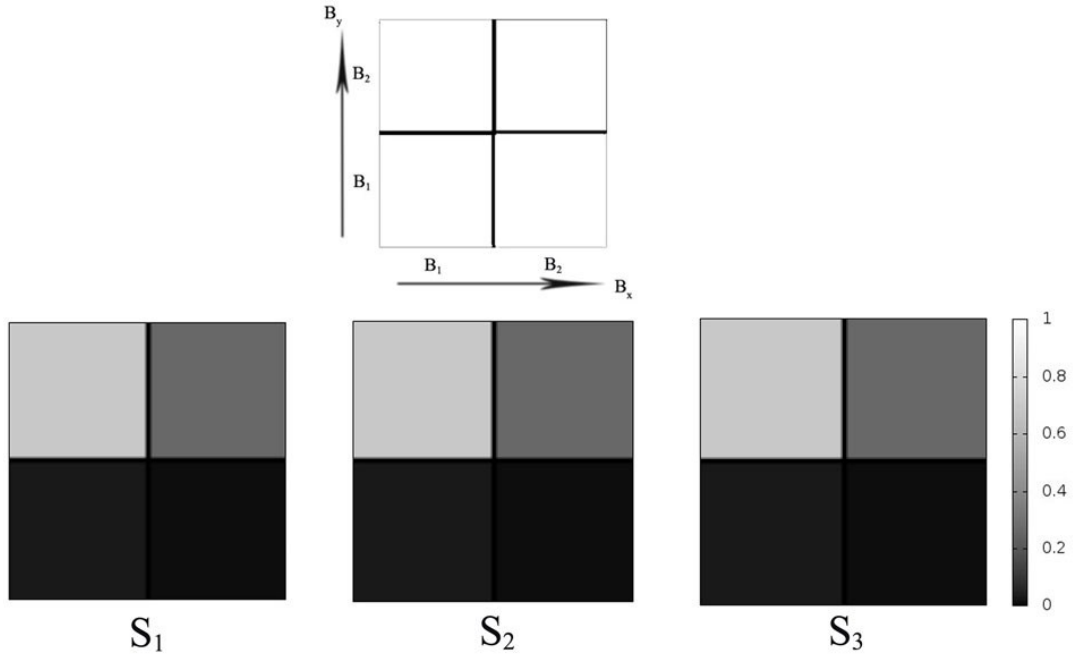

Fig. S2 Transition density analysis for S_1, S_2 and S_3 state at the ground state geometry of the $[Cu(dmp)_2]^+$ complex. The classification of electronic transition within two blocks, namely, the copper (B_1) and the ligands (B_2). Each square stands for the transition from the B_x (horizontal) to B_y (longitudinal) blocks (see the top panel). The color codes in this Figure indicate the amplitude of transition intensity.

In our studies, the geometry of $[Cu(dmp)_2](PF_6)$ complex was optimized with a few DFT functionals, including BHandHLYP, CAM-B3LYP, M06-2X. And only minor structural difference is observed. We also optimized geometry of $[Cu(dmp)_2](PF_6)$ complex with the dispersion corrected functional (wB97XD). And the optimized geometries are very similar, which can be rationalized by the fact that the electrostatic interaction is dominated in the case of the $[Cu(dmp)_2](PF_6)$ complex.

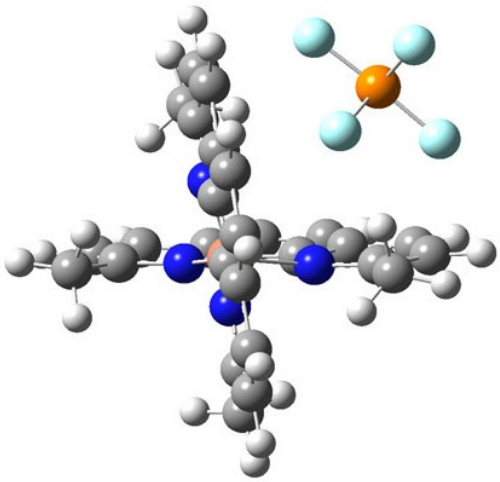

Fig. S3 The local minima for the ground state of $[Cu(dmp)_2](PF_6)$. The optimization was performed with a few DFT functionals (BHandHLYP, M06-2X, CAM-B3LYP, and wB97XD), and the structural difference is minor. The optimized interligand dihedral angle (φ) was in the range of 83~86°.

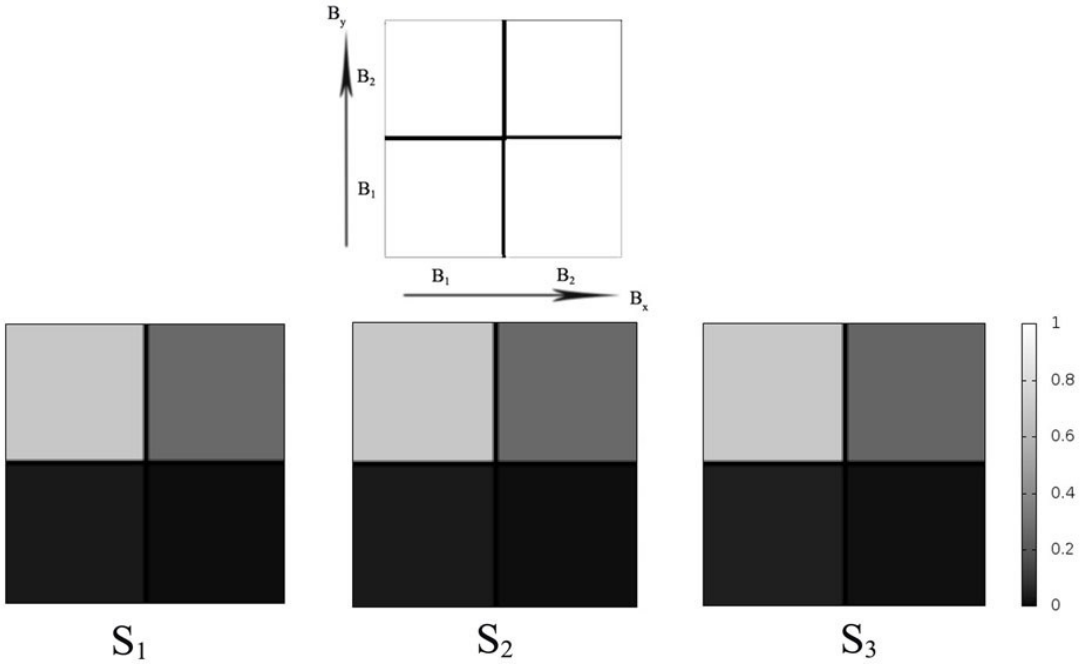

Fig. S4 Transition density analysis for S_1, S_2, and S_3 state at the ground state geometry of the $[Cu(dmp)_2](PF_6)$ complex. The classification of electronic transition within two blocks, namely, the copper (B_1) and the ligands (B_2). Each square stands for the transition from the B_x (horizontal) to B_y (longitudinal) blocks (see the top panel). The color codes in this Fig. indicate the amplitude of transition intensity.

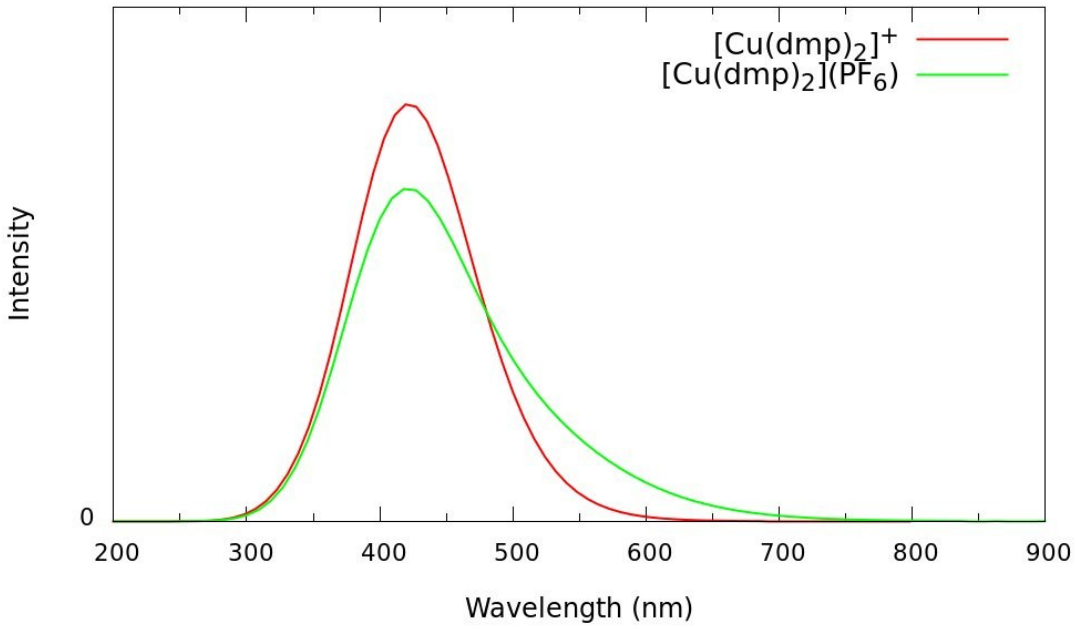

Fig. S5 The UV-vis absorption spectra for the $[Cu(dmp)_2]^+$ and $[Cu(dmp)_2](PF_6)$ complex. The absorption spectrum was calculated at TDDFT level by collecting the oscillation strength at the corresponding transition energy over a large number of sampled geometries. The CAM-B3LYP/6-31G* method was used, and the Gaussian broadening with FWHW of 0.2 eV is applied.

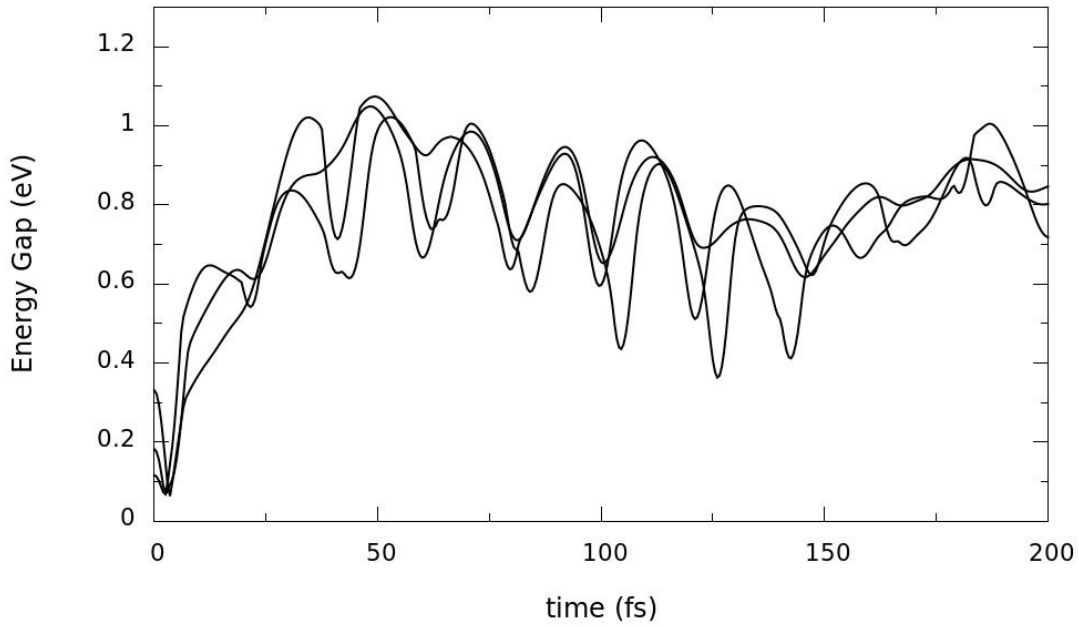

Fig. S6 Time evolution of the energy gap between S_2 and S_3 for three typical trajectories. The small energy gap at the initial stage of the dynamics is observed.

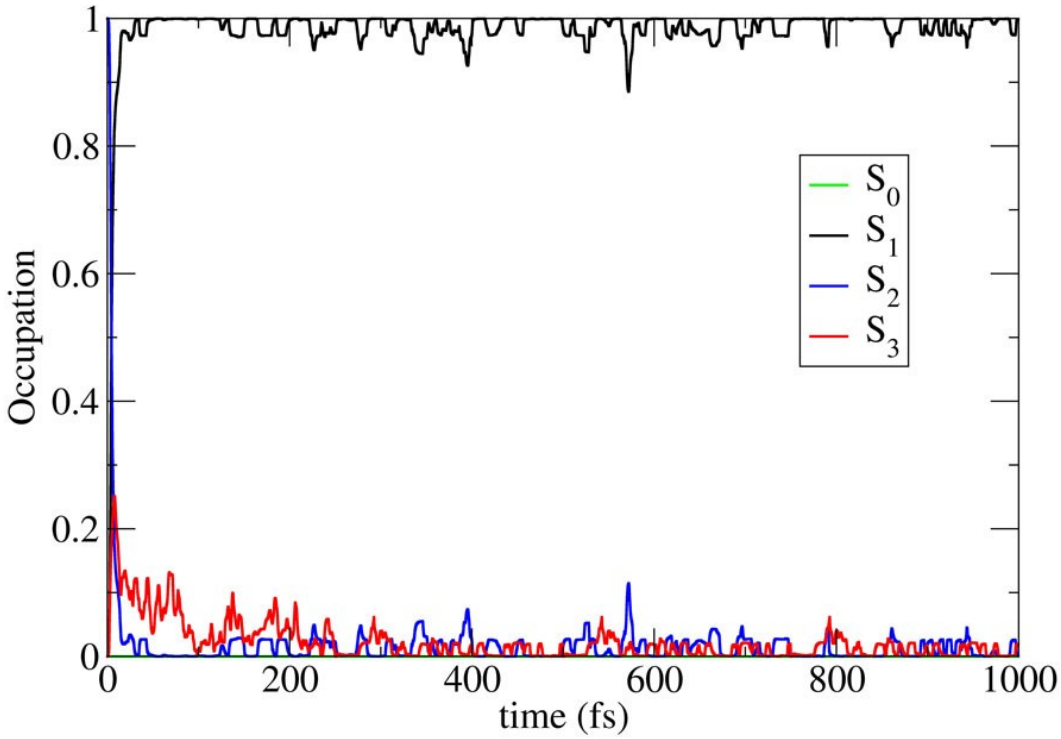

Fig. S7 (a) The average fractional occupation of trajectories for each state starting at S_2 state calculated at the TDDFT/CAM-B3LYP level.

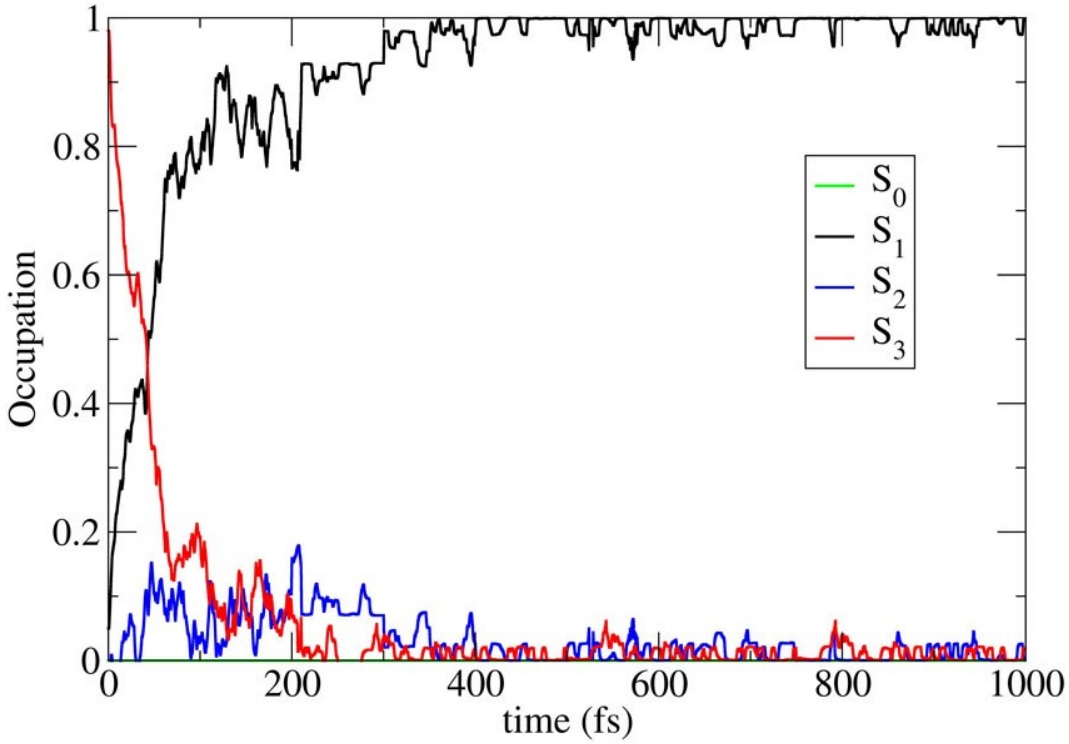

Fig. S8 (a) The average fractional occupation of trajectories for each state starting at S_3 state at the TDDFT/CAM-B3LYP level.

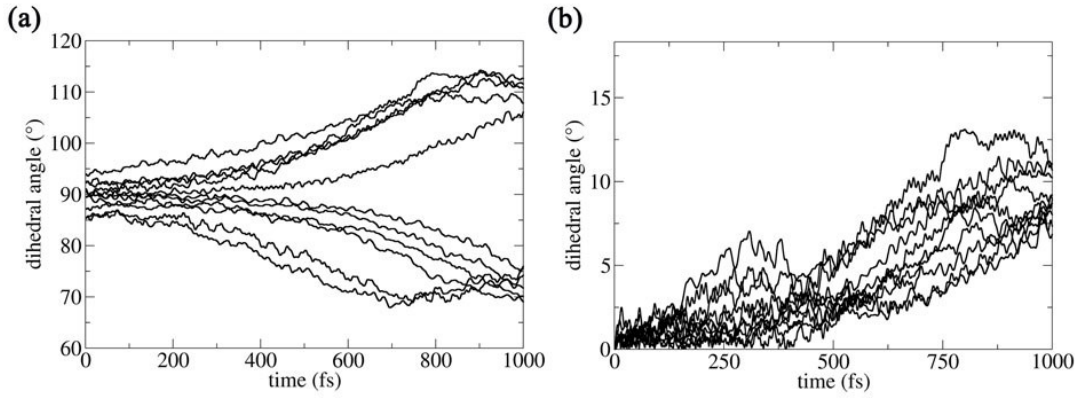

Fig. S9 (a) Time evolution of the interligand dihedral angle (φ) for several specific trajectories; (b) The dihedral angle of one dmp ligand with respect to its initial frame, as a function of time, for 10 specific trajectories.

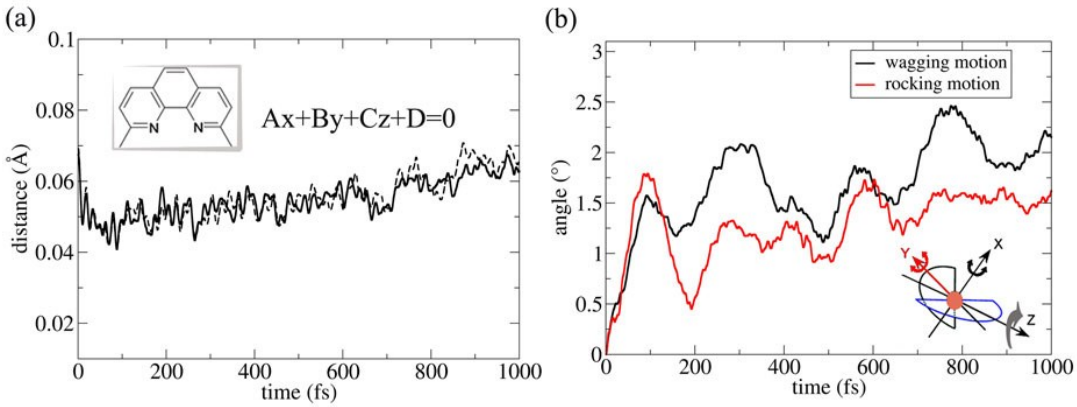

Fig. S10 (a) Time-dependent deviation of a dmp ligand from its corresponding planar equation, which is described by the residue from the planar equation. Note that the hydrogen atoms were omitted in our analysis; (b) time-dependent wagging (X axis) and rocking (Y axis) motions.